

1 **Quantification of Aquatic Unicellular Diazotrophs by Immunolabeled Flow**  
2 **Cytometry**

3 **Eyal Geisler<sup>1,2\*</sup>, Hagar Siebner<sup>1</sup>, Eyal Rahav<sup>2</sup>, Edo Bar-Zeev<sup>1\*</sup>**

4 <sup>1</sup>Zuckerberg Institute for Water Research, Jacob Blaustein Institutes for Desert  
5 Research, Ben-Gurion University of the Negev, Sede Boqer Campus, 84990, Israel.

6 <sup>2</sup>Israel Oceanographic and Limnological Research, National Institute of  
7 Oceanography, Haifa, 31080, Israel.

8

9 \* **Corresponding authors:** Edo Bar-Zeev, [barzeeve@bgu.ac.il](mailto:barzeeve@bgu.ac.il) and Eyal Geisler,  
10 [geisler@post.bgu.ac.il](mailto:geisler@post.bgu.ac.il)

11 **Key Words:** Flow cytometry, Immunolocalization, Diazotrophs, N<sub>2</sub> fixation,  
12 Bacterial abundance

13

14 **Conflict of interest statement:** The manuscript is original and have not been submitted  
15 elsewhere for consideration. There is no conflict of interest and all co-authors have seen  
16 and approved the current version for submission.

17

18

19

20

21

## 22 **Abstract**

23 Quantifying the number of aquatic diazotrophs is highly challenging and relies mainly  
24 on microscopical approaches and/or molecular tools that are based on *nif* genes.

25 However, it is still challenging to count diazotrophs, especially the unicellular  
26 fraction, despite their significant contribution to the aquatic nitrogen cycle. In this  
27 study a new method was developed to quantify unicellular diazotrophs by  
28 immunolabeling the nitrogenase enzyme followed by identification and quantification  
29 via flow cytometry. The new quantification method was initially developed using a  
30 diazotrophic monoculture (*Vibrio natriegens*) and verified by various auxiliary  
31 approaches. It was found that only 15-20% of the total number of *V. natriegens* cells  
32 have synthesized the nitrogenase enzyme, even though the media was anaerobic, and  
33 N limited. This approach was further tested in samples from marine and freshwater  
34 environments. It was found that the ratio of diazotrophs to total bacteria was 0.1% in  
35 the Mediterranean Sea, while 4.7% along the Jordan River. In contrast, the specific N<sub>2</sub>  
36 fixation per unicellular diazotrophs was highest in the Mediterranean Sea (88 attomole  
37 N cell<sup>-1</sup> d<sup>-1</sup>) while the total N<sub>2</sub> fixation rates were lowest in the lake and the river (0.2  
38 nmole N L<sup>-1</sup> d<sup>-1</sup>). Overall, we expect that this direct quantification approach will  
39 provide new insights on the number and contribution of unicellular diazotrophs to  
40 total N<sub>2</sub> fixation in marine and freshwater environments under various conditions.

41

42

43

44

45

## 46 **Introduction**

47 Biological N<sub>2</sub> fixation is a central process in marine and freshwater environments as it  
48 supplies new nitrogen compounds and support primary production (Gruber &  
49 Galloway, 2008; Zehr & Capone, 2020). Dinitrogen fixation is carried by a specific  
50 subgroup of bacteria and archaea known as diazotrophs. These organisms use the  
51 nitrogenase enzyme, a two-component complex comprised MoFe protein and Fe-  
52 reductase protein (Hoffman et al., 2014). Studies have indicated that aquatic  
53 diazotrophs include autotrophic (Zehr, 2011), heterotrophic (Bombar et al., 2016;  
54 Riemann et al., 2010) and mixotrophic (Benavides et al., 2020; Feng et al., 2010)  
55 metabolism to maintain the energetic requirements of the nitrogenase enzyme.  
56 Aquatic diazotrophs can be found in benthic mats, organized in long filamentous  
57 chains (up to few hundreds of micrometers), free living planktonic cells, or associated  
58 with aggregates (Bergman et al., 2013; Bertics et al., 2010; Riemann et al., 2022).  
59 Quantifying the abundance of aquatic diazotrophs, especially the unicellular fraction,  
60 is challenging, thus missing in most ecological studies, despite their biochemical  
61 importance. Traditionally, microscopical approaches were used to count diazotrophs,  
62 for most part filamentous bacteria such as *Trichodesmium* sp. and *Anabena* sp.  
63 (Spungin et al., 2016; Zulkefli & Hwang, 2020). During the last two decades various  
64 molecular methods such as quantitative polymerase chain reaction were also used to  
65 estimate the numbers of smaller, unicellular diazotrophs (Foster et al., 2007; Turk et  
66 al., 2011). These methods are mostly based on evaluating the numbers of diazotrophs  
67 focus on the potential transcription (DNA) or expression (mRNA) of *nifH* genes.  
68 Previous studies have immunolabeled the nitrogenase enzyme to visualize aquatic  
69 diazotrophs (Currin et al., 1990; Geisler et al., 2019; Lin et al., 1998) . Differently  
70 than targeting the *nifH* gene, it was estimated that diazotrophs which synthesized the

71 nitrogenase enzyme are likely to actively fix dinitrogen. However, the advantages of  
72 nitrogenase immunolabeling for unicellular diazotrophs quantification was yet  
73 developed.

74 In this study nitrogenase immunolabeling was compiled with flow cytometry to  
75 quantify the number of unicellular diazotrophs in aquatic environments. The  
76 quantification method is based on immunolabeling the MoFe subunit of the  
77 nitrogenase enzyme by two antibodies conjugated to a green fluorophore. The method  
78 was first calibrated with *Vibrio natriegens* as a representative unicellular diazotrophs  
79 and then validated in-situ from several marine and freshwater environments.  
80 Complimentary N<sub>2</sub> fixation measurements were undertaken, enabling to quantify the  
81 diazotrophic cell-specific activity.

## 82 **Materials and Methods**

### 83 *Culturing unicellular diazotroph and non-diazotrophic bacteria*

84 *Vibrio natriegens* (ATCC 14048) and/or *Escherichia coli* (ATCC 11303) were  
85 acclimated in a gas tight bottles (100 ml) containing Luria Bertani Broth media (LB,  
86 Merck Millipore, BD, 0083370) under anaerobic conditions ( $\sim 0.2$  mg L<sup>-1</sup> O<sub>2</sub>) at 26 °C  
87 overnight. The LB media used to grow the *V. natriegens* also included 1.5 % NaCl  
88 (Sigma Aldrich, 312525). Cells were further diluted to  $\sim 5 \times 10^6$  cells ml<sup>-1</sup> and re-grown  
89 to a mid-logarithmic phase with an  $\sim 2 \times 10^8$  cells ml<sup>-1</sup> for 1-2 h under the same  
90 conditions. Bacterial cells were centrifuged (3500 g for 6 min) to remove the LB and  
91 resuspended in artificial brackish water (1 ml) to a final cell concentration of  $\sim 2 \times 10^6$   
92 cells ml<sup>-1</sup>. The chemical composition of the artificial media is detailed in the  
93 supporting information.

94 Triplicate biological replicates containing either *V. natriegens*, *E. coli* or both (1:1)  
95 were resuspended in N limited brackish water, enriched with  $^{15}\text{N}_2$  (99%, Cambridge  
96 Isotopes, lot #NLM-363-PK, final concentration 1% v:v). Monocultures or mixed  
97 cultures were then incubated for 48 hours under dark and anoxic conditions at 26 °C.  
98 Additional two bottles from each bacterial type were not enriched with  $^{15}\text{N}_2$  to  
99 determine their natural isotopes ratio. At the conclusion of the incubation, sub  
100 samples were analyzed for  $\text{N}_2$  fixation rates, colony forming units (CFU), as well as  
101 total bacterial abundance (BA) and diazotrophic abundance (DA) as detailed below.  
102 In addition, diazotrophs were visualized by capturing immunolabeled subsamples by  
103 confocal laser scanning microscopy (CLSM).

#### 104 *Collection of natural diazotrophs*

105 Surface waters were collected from three sampling locations, the South Eastern  
106 Mediterranean Sea, Qishon Estuary, and Sea of Galilee Lake (Table S1). Water were  
107 incubated in 1 L Nalgene bottles.  $\text{N}_2$  fixation rates were determined by enriching the  
108 samples with 15 % of dissolved  $^{15}\text{N}_2$  stock. Enriched samples were incubated for 48 h  
109 at room temperature under 12h light/dark conditions. Subsamples (1.7 ml) were  
110 collected at the end of the incubation for BA and DA analysis as well as diazotroph  
111 microlocalization.

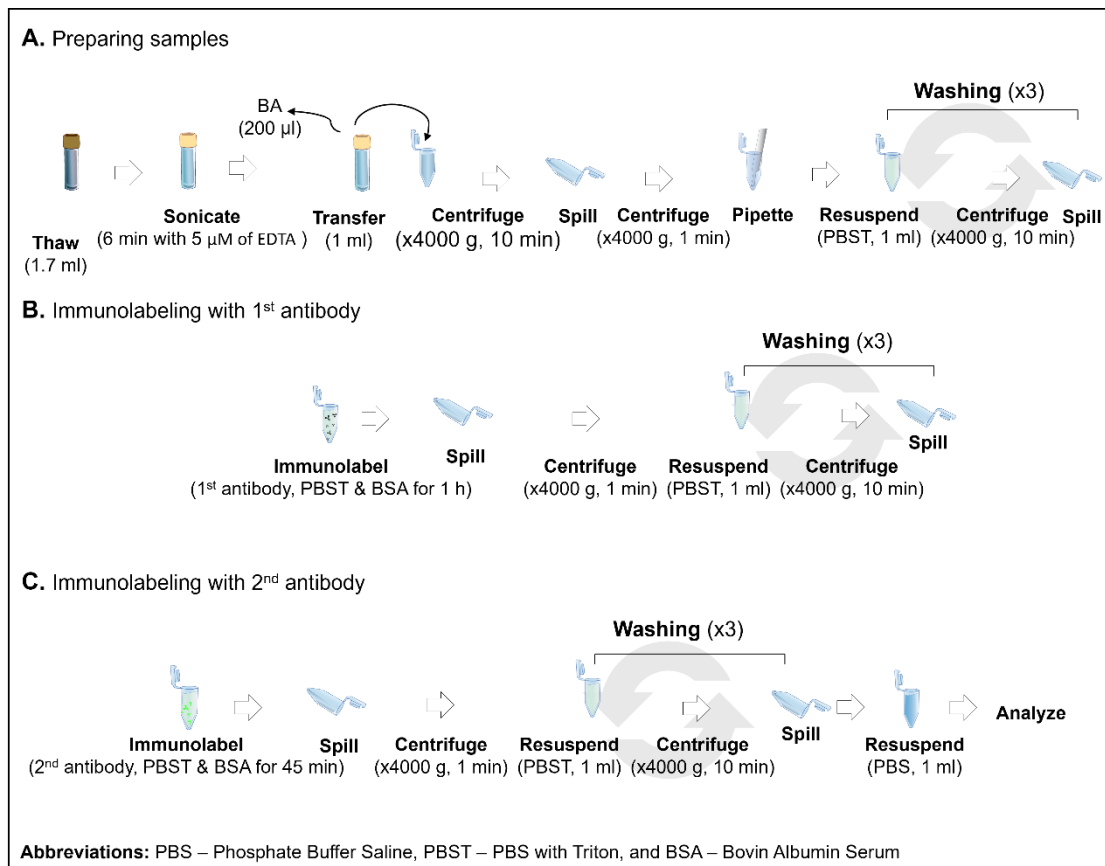
#### 112 *Analytical methods*

##### 113 *Diazotrophs immunolabeling for flow cytometric analysis*

114 Monoculture and natural samples (1.7 ml) were fixed with 50% glutaraldehyde (final  
115 concentration, 0.2 % Sigma-Aldrich, G7651), flash frozen in liquid nitrogen and  
116 stored at -80 °C until analyses. Samples were prepared by slow thawing at room  
117 temperature (Figure 1A). Next, ethylenediaminetetraacetic acid (EDTA, Sigma

118 Aldrich, 03690) was added (final concentration of 5  $\mu\text{M}$ ) to chelate cations and  
119 facilitate aggregates dispersion (Bogler & Bar-Zeev, 2018). Samples were also  
120 sonicated in a bath sonicator for 6 min to disassociate cells from the aggregate matrix  
121 and one another. Subsamples (1 ml) were transferred and centrifuged for 10 minutes  
122 at x4000 g (a subsample was also collected for total bacterial abundance, detailed are  
123 provided below). The supernatant was cautiously discarded to maintain the bacterial  
124 pellet. Wash solution was prepared by mixing phosphate buffer saline (PBS) and  
125 Triton X-100 (T, final concentration of 0.1 %, Sigma Aldrich, X100), define hereafter  
126 as PBST. The wash solution was added to perforate the cell envelope. Samples were  
127 centrifuged for 10 minutes at x4000 g, while the supernatant was cautiously  
128 discarded. This washings-centrifugal cycle was repeated three times to increase the  
129 efficiency of cellular perforation. Fresh anti-nitrogenase antibody (3  $\mu\text{g ml}^{-1}$ , Agrisera  
130 Antibodies AS01 021A) was prepared with PBST and bovine albumin serum (BSA,  
131 filtered 0.2  $\mu\text{m}$ , 1  $\text{mg ml}^{-1}$ , Sigma Aldrich A2153) to minimize unspecific antibody  
132 binding (Figure 1B). Samples were then incubated while slowly rotating (Benchmark  
133 Scientific Roto-Therm Plus, H2024) for one hour at room temperature to  
134 facilitate binding between the nitrogenase MoFe subunit and the primary antibody.  
135 Unbonded antibodies were removed by washing the samples three times with PBST  
136 similarly to the above. Washed samples were then incubated at room temperature in  
137 the dark for 45 min with the secondary antibody (3  $\mu\text{g ml}^{-1}$ , Thermo Fisher Scientific  
138 A-11039) conjugated to a green fluorophore (Alexa Fluor™ 488) with Ex spectra of  
139 498 nm and Em of 520 nm (Figure 1C). Any untagged residues of the secondary  
140 antibodies were removed by washing the samples three times with PBST as described  
141 above. Immunolabeled samples were suspended with sterile PBS (1 ml) without any  
142 additions. Additionally, few controls were prepared following the above procedure

143 and tested to evaluate the specific tagging of diazotrophs: (1) Negative control,  
144 namely PBST-BSA without any antibodies, to determine whether any  
145 autofluorescence could be detected; (2) no addition of the 1<sup>st</sup> antibody (PBST-BSA  
146 with the 2<sup>nd</sup> antibody only); and (3) no addition of the 2<sup>nd</sup> antibody (PBST-BSA with  
147 the 1<sup>st</sup> antibody only) to verify if any unspecific adsorption occurred. Additional  
148 control was to test unspecific tagging by applying the immunolabeling approach on  
149 non-diazotrophic (*E. coli*) bacteria. It should be noted that after each washing stage a  
150 subsample (100  $\mu$ l) was collected to count the number of bacteria that were lost  
151 (Figure S1).



152

153 **Figure 1.** Graphical summary of the immunolabeling stage for flow cytometric  
154 analysis. The method is divided into three main stages: sample preparation (A);  
155 Immunolabeling with the 1<sup>st</sup> antibody (B) and tagging with the 2<sup>nd</sup> antibody  
156 conjugated to the green fluorophore (C).

157 *Counting immunolabeled diazotrophs and total bacteria using flow cytometry*

158 Diazotroph abundance (DA) was determined by detecting and counting  
159 immunolabeled subsample (200  $\mu$ l) using Attune-Next acoustic flow cytometer  
160 (Applied Biosystems). Changes in the abundance of monoculture diazotrophs were  
161 determined after diluting the immunolabeled samples (1:100, 1:250, 1:500, 1:1000).  
162 Monocultures were analyzed at a flow rate of 100  $\mu$ l  $\text{min}^{-1}$ , while reduced to 25  $\mu$ l  
163  $\text{min}^{-1}$  for natural samples. Stop condition was set to 20,000 counts for all samples.  
164 Calibration beads (1  $\mu$ m, F8815, Invitrogen, Ex: 350 nm Em: 440 nm) were added  
165 (final concentration of  $1.8 \times 10^4$  beads  $\text{ml}^{-1}$ ) every 12 samples to evaluate the size  
166 spectrum of the sample.

167 Following the above, total bacterial abundance (BA) was quantified by staining non-  
168 immunolabeled subsamples (200  $\mu$ l) with SYBR Green I (S7563, Invitrogen, final  
169 concentration, 1 nM) (Geisler et al., 2019). Samples were incubated for 15 min under  
170 dark conditions. Stained samples were measured with Attune-Next Acoustic Flow  
171 Cytometry. MilliQ (sterile) water samples were used to clean the system every five  
172 samples, while PBS were tested and subtracted as blanks. The specified lasers, dyes  
173 and filters are detailed in table 1.

174 **Table 1.** Analytical specifications of the flow cytometer.

Parameter	Laser (nm)	Excitation (nm)	Emission (nm)	Detector (nm)
Side scattering (SSC)	450 (Blue)	450	-	488 $\pm$ 10
SYBR GREEN I	450 (Blue)	497	520 (Green)	520 $\pm$ 30
Nitrogenase Immunolocalization	450 (Blue)	500	520 (Green)	520 $\pm$ 30

175

176



177 *Quantifying cells using colony forming units (CFU) counts*

178 Samples were collected from the incubation bottles and serially diluted in parallel to  
179 the immunolabeled samples (1:100, 1:250, 1:500, 1:1000). Subsamples (25  $\mu$ l) were  
180 plated on an agar plate (1.5%, Bacto Agar, DF0140) with an N limited brackish water  
181 media (the recipe is detailed in the supporting information). CFU samples were  
182 incubated under anaerobic conditions for 48 hours at 26 °C. CFU were determined at  
183 the end of the incubation by counting plates with 30-300 colonies.

184

185 *Microlocalization of diazotrophs using confocal laser scanning microscopy (CLSM)*

186 Immunolabeled samples (50  $\mu$ l) were stained with 250  $\mu$ g ml<sup>-1</sup> of 4',6-Diamidino-2-  
187 Phenylinidole (DAPI, Ex 360 nm and Em 460 nm, Thermo Fisher, D1306) or (SYBR  
188 Green I, Ex 497 nm and Em 520 nm) and incubated for 20 minutes under dark  
189 conditions. Samples were drop-casted on a glass microscope slide, sealed by a cover  
190 slide and nail polish to minimize dehydration. Immunolabeled nitrogenase enzyme  
191 was visualized by a CLSM 900 equipped with a 488 nm laser (Power, 0.2 % digital  
192 gain, ~500 V, pinhole, 32  $\mu$ m). Stained bacteria were visualized with a 405 nm laser  
193 (Power, 0.9 %, digital gain, ~730 V and pinhole, 37  $\mu$ m). Samples were observed  
194 under a x63 lens (63x/1.4 Oil DIC M27, respectively). Non stained samples were used  
195 before to identify and subtract autofluorescence. Images were processed using Zeiss  
196 ZEN Blue edition (3.5, lite, Germany).

197

198

199

200 *Measuring N<sub>2</sub> fixation rates*

201 Samples were filtered on a pre-combusted glass microfiber filter (GF/F, Cytivia,  
202 1825025, 450 °C, 4.5 h) after 48h incubation in <sup>15</sup>N<sub>2</sub> enriched media. Different  
203 volumes of samples (25 ml for lab cultures and 1L for environmental microcosms)  
204 were filtered, to ensure sufficient biomass (resulting in an amplitude of ~1000 mv) on  
205 the filter as their source varied from monocultures to different natural environments.  
206 Samples were dried in the oven overnight (60 °C) and stored in the desiccator until  
207 measurements. Filters were carefully packed in tin capsules, with clean, pre-  
208 combusted glass fiber (GF/F) filters used as blanks. The samples were then analyzed  
209 using elemental analyzer (EA; Thermo Scientific, Flash 2000 HT) coupled with  
210 isotope ratio mass spectrophotometer (IRMS; Thermo Scientific, Delta V Plus).  
211 Working with filters and environmental samples over a wide range of concentrations  
212 requires caution during the isotopic measurement. The quality control measures taken  
213 during the measurement are detailed in the supporting information. Briefly: Three  
214 standards (Glutamic Acid USGS 40, Glycine USGS 64, and Caffeine USGS 62) were  
215 chosen for calibration, bracketing the expected range for δ<sup>15</sup>N of the enriched, as well  
216 as natural abundance samples, and ensure accuracy (Figure S2A). Acetanilide  
217 (Thermo Scientific, BN240741) was used for linearity test over the measured range  
218 (Figure S2B) and for quantitative calibration of peak amplitude vs. μg N in sample's  
219 biomass (Figure S2D). A working range of 10 to 55 μg N per sample was determined  
220 to assure precision and avoid linearity effect. Similar ranges of nitrogen (> 10 μg N  
221 per filter) were previously determined (White et al., 2020). No drift was measured  
222 (slope = 0.01) and good precision was found (±0.3‰) throughout the analysis (Figure  
223 S2C). The natural abundance of <sup>15</sup>N, reflected by the ratio of <sup>14</sup>N/<sup>15</sup>N in each culture  
224 or environmental sample, was subtracted from that of the corresponding enriched

225 sample to calculate N<sub>2</sub> fixation rates, according to previous reports (Montoya et al.,  
226 1996).

### 227 *Statistical analyses*

228 Statistical tests were ran using XLSTAT (2022.2, New-York). Before analyses,  
229 normal distribution of the data was validated using Shapiro Wilk test. The links  
230 between BA, DA, CFU and N<sub>2</sub> fixation were measured by a Pearson correlation test.  
231 For comparing N<sub>2</sub> fixation and BA/DA between samples, Analysis of Variance  
232 (ANOVA) was used with post-hoc Tukey test. All the tests were run under the  
233 confidence level of 95 % ( $\alpha=0.05$ ).

234

## 235 **Results and Discussion**

### 236 **Detecting and quantifying a unicellular diazotrophic monoculture**

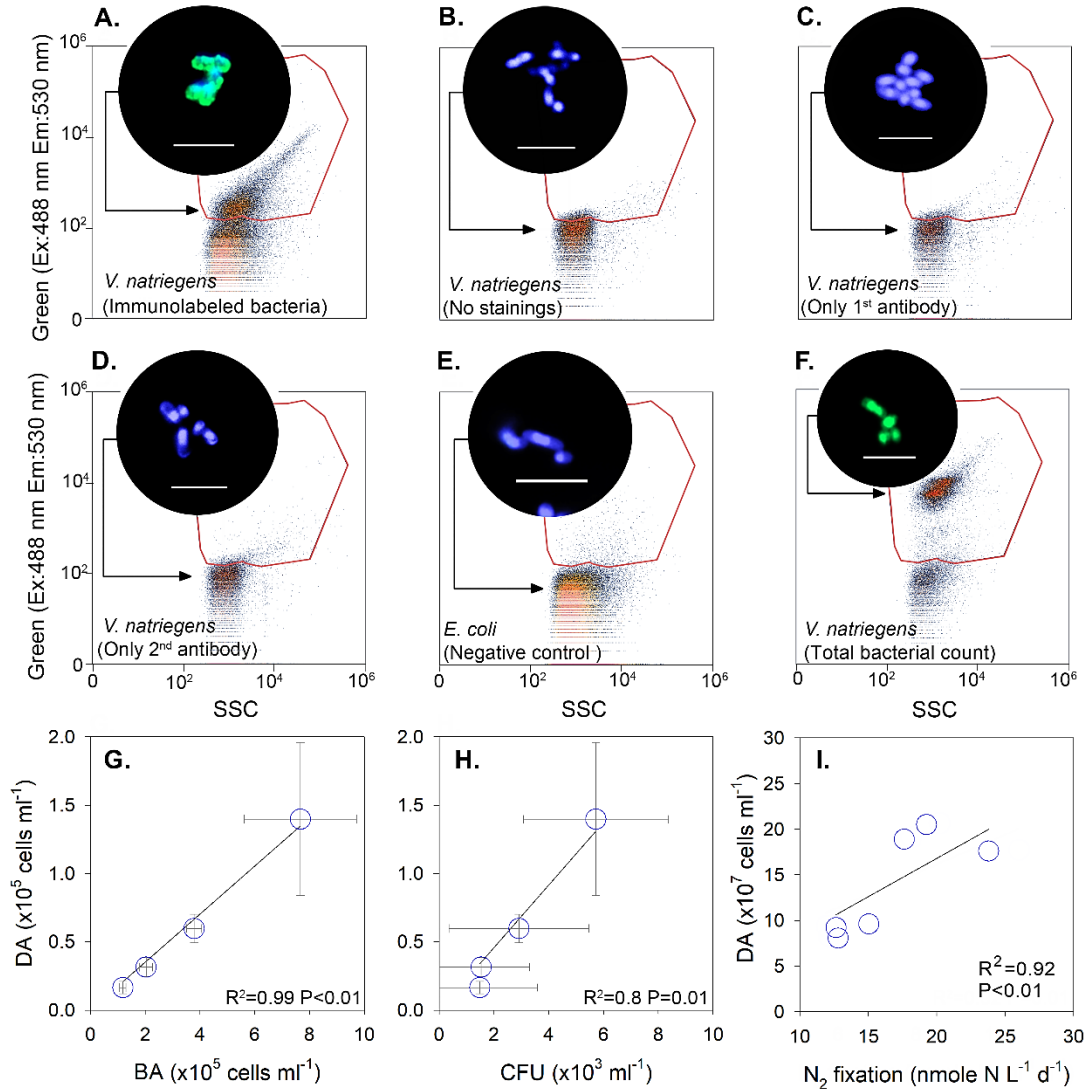
237 Immunolabeled *V. natriegens* formed a distinct cluster after analyzing the samples by  
238 flow cytometry using a green detector over side scatter (Figure 2A). In contrast, only  
239 few unlabeled cells (< 1000 events) were captured in the same region (Figure 2B).  
240 Similarly, no *V. natriegens* cells were detected after tagging with the first or the  
241 second antibodies only (Figure 1C-D). Following the above, only conjunction of the  
242 two antibodies led to a positive detection of *V. natriegens* by flow cytometry,  
243 excluding any autofluorescence or unspecific adsorption of the tags to the cells.  
244 Finally, no immunolabeling by non-diazotroph, *E. coli* bacteria were detected in the  
245 region of interest by the flow cytometer (Figure 2E). The negative control highlighted  
246 that only cells with the nitrogenase enzyme could be tagged by the antibodies and  
247 detected as previously reported in other studies (Chelius & Triplett, 2000; Geisler et  
248 al., 2019).

249 Total bacterial abundance was counted in an independent test after tagging a  
250 subsample with a nucleic acid stain (SYBR green) only. Tagging bacteria with SYBR  
251 green resulted in a distinct cluster that was identified in the same region of interest as  
252 described above (Figure 2F) and similar to previous studies (e.g., Geisler et al., 2019).  
253 Complimentary visualization of *V. natriegens* and *E. coli* subsamples by CLSM  
254 confirmed the results detected by the flow cytometry (Figure 2, circles).

255 Linear and significant correlation was detected between the number of  
256 immunolabeled *V. natriegens* and the total number of cells tagged by SYBR green  
257 from the same monoculture (Figure 2G). That trend line indicates that between 15 %  
258 to 20% of all *V. natriegens* bacteria were specifically tagged by immunolabeling,  
259 namely the cells that synthesized the nitrogenase enzyme. Correspondingly, a linear  
260 correlation was also found between immunolabeled cells and CFU counts that grew  
261 on limited nitrogen agar plates under anaerobic conditions for 48h (Figure 2H). It  
262 should be noted that the number of immunolabeled cells detected by flow cytometry  
263 was 20-25 times higher than those counted on the agar plates. In addition, a linear  
264 relationship was found between the number of *V. natriegens* that synthesized the  
265 nitrogenase enzyme and N<sub>2</sub> fixation rates (Figure 2I), resulting in a specific N<sub>2</sub>  
266 fixation per cell of  $1.3 \pm 0.3$  attomole N cell<sup>-1</sup>.

267 Lower percentage of free living diazotrophs that synthesized the nitrogenase enzyme  
268 compared to total cell count may indicate that heterotrophic N<sub>2</sub> fixation was partly  
269 suppressed even under anerobic conditions and limited concentrations of inorganic  
270 nitrogen (confirmed also by low fixation rates per cell). Although the scope of the  
271 study was to develop a new quantification method for diazotrophs, it could be  
272 surmised that other constraints that were not measured such as pH (Luo et al., 2019)

273 and/or carbon liability (Benavides et al., 2020; Rahav et al., 2016) impaired N<sub>2</sub>  
274 fixation.



275

276 **Figure 2.** Representative density plots of the main verification tests (A-F) and  
277 correlation charts of the corresponding quantification results (G-I). The region of  
278 interest for immunolabeled *V. natriegens* diazotrophs as well as total bacterial count  
279 (individually tested after nucleic staining) was determined according to green  
280 fluorescence over side scatter (SSC). Diazotrophic abundance (DA) was correlated to  
281 total bacterial abundance (BA) (G) as well as colony forming units (CFU) (H) and N<sub>2</sub>  
282 fixation rates (I). Top circles of each plot (A-F) capture subsample images using  
283 confocal laser scanning microscope with a scale bar of 5 μm. Diazotrophs were  
284 identified by nitrogenase immunolabeling (Green) while all the cells were detected by

285 DAPI (Blue) or SYBR green (Green). Additional images are provided in supporting  
286 information (Figure S3A-E).

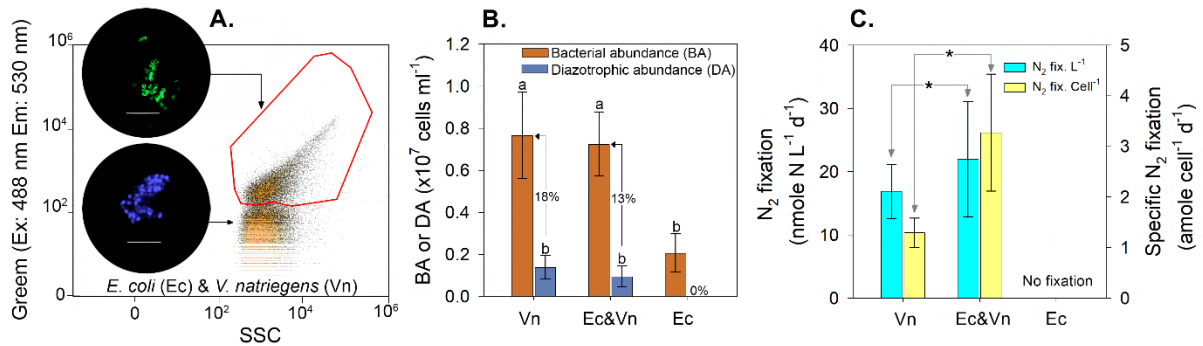
### 287 **Counting diazotrophic and non-diazotrophic mixed cultures**

288 Two monocultures that included a diazotrophic (*V. natriegens*) and a non N<sub>2</sub> fixing  
289 bacteria (*E. coli*) were mixed to test the differentiation capacity of the new  
290 immunolabeled—flow cytometry-based approach. Staining the DNA of subsamples  
291 with SYBR green for total bacterial count formed a distinct cluster (Figure 2F).  
292 Immunolabeling diazotrophic monoculture as well as a mixture of *V. natriegens* and  
293 *E. coli* bacteria resulted in a clear cluster over the conjugated nitrogenase (green)  
294 threshold (Figure 3A).

295 Quantifying total bacteria indicated that the numbers of *V. natriegens* only as well as a  
296 mixture with *E. coli* were similar ( $\sim 0.75 \times 10^7$  cell ml<sup>-1</sup>) after 48 h of anaerobic  
297 incubation in a nitrogen limited media. It should be noted that the number of *E. coli*  
298 cells in a monoculture was lower by 71% (Figure 3B). Counting the immunolabeled  
299 cells indicated that the number of N<sub>2</sub> fixing diazotrophs, namely *V. natriegens* that  
300 synthesized the nitrogenase enzyme, constitute 18% of the total *V. natriegens* cells  
301 and 13% of the mixed culture. Note, no immunolabeled *E. coli* cells were detected by  
302 the flow cytometer (Figure 3B), ruling out any unspecific links or adsorption of the  
303 fluorophore.

304 Corresponding N<sub>2</sub> fixation rates were found to be significantly higher (1.3 times) by  
305 *V. natriegens* mixed with *E. coli* than in the monoculture (Figure 3C). That difference  
306 was even greater (2.5 times) when comparing N<sub>2</sub> fixation rates per cell in the mixed  
307 culture to those measured from the *V. natriegens* culture. Altogether, it appears that  
308 mixing *V. natriegens* with a non diazotrophic heterotrophic bacteria such as *E. coli*  
309 spur N<sub>2</sub> fixation rates per cell. It is plausible that increasing N<sub>2</sub> fixation rates per cell

310 enabled *V. natriegens* to compensate the enhanced consumption of limited dissolved  
311 inorganic nitrogen (initial concentration of 80  $\mu\text{M}$ ) that was included in the artificial  
312 media.



313

314 **Figure 3.** Representative flow cytometry plot of *E. coli* (Ec) and *V. natriegens* (Vn)  
315 mixed culture (A). The corresponding CLSM micrographs capture immunolabeled  
316 diazotrophs (5  $\mu\text{m}$  scale bar). Additional image is provided in supporting information  
317 (Figure S3F). Abundance of non (*E. coli*) and diazotrophic bacteria (*V. natriegens*) in  
318 mono and mixed cultures was quantified after DNA staining and nitrogenase  
319 immunolabeling by flow cytometry (B). Corresponding  $\text{N}_2$  fixation rates were  
320 determined from all the cultures (C).  $\text{N}_2$  fixation rates per cell were calculated by  
321 normalizing the measured rates to the number of immunolabeled diazotrophs counted  
322 in the same culture. Values represent the mean and standard deviation from six  
323 independent replicates. Letters above the bars refer to ANOVA analysis followed by a  
324 Tukey post hoc test.

325

### 326 Evaluating the abundance of unicellular diazotrophs in aquatic environments

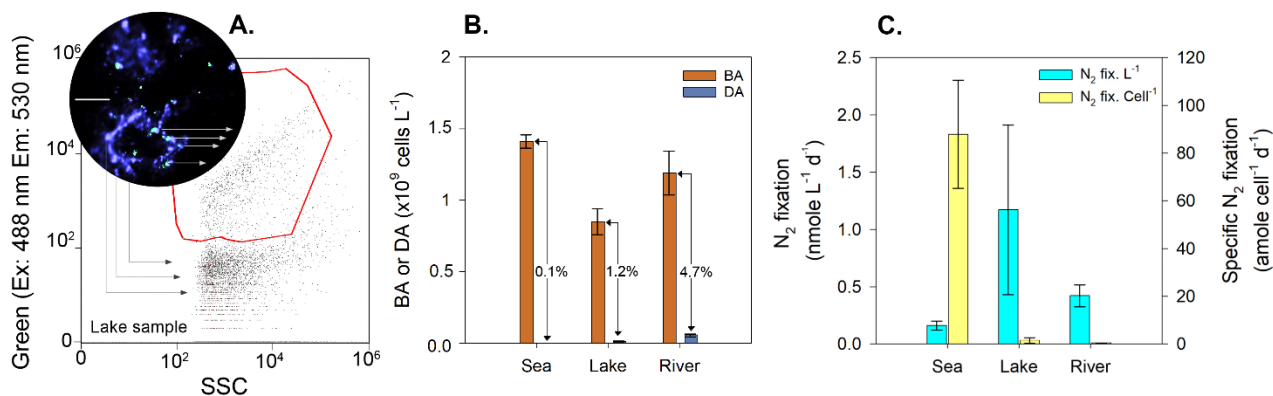
327 Quantification of unicellular diazotrophs from different aquatic environments by  
328 immunolabeled flow cytometry resulted in a marked cluster, yet slightly more  
329 scattered than the monoculture controls (Figure 4A). Complimentary imaging of  
330 subsamples by CLSM indicated that only a small fraction of the cells collected from

331 the Sea of Galilee Lake were tagged by nitrogenase immunolabeling (Figure 4A, top  
332 circle).

333 Sporadic collection of water samples from different aquatic environments indicated  
334 that the abundance of unicellular diazotrophs ranged from  $2 \pm 0.2 \times 10^7$  cells L<sup>-1</sup> in the  
335 Mediterranean Sea to  $1 \pm 0.7 \times 10^7$  cells L<sup>-1</sup> in the Sea of Galilee Lake and  $6 \pm 0.9 \times 10^7$   
336 cells L<sup>-1</sup> in the Jordan River. The number of diazotrophs found in these environments  
337 were between 0.1% to 4.7% out of the total bacterial abundance (Figure 4B).

338 Corresponding N<sub>2</sub> fixation rates from these samples were between 0.2 to 1.2 nmole N  
339 L<sup>-1</sup> (Figure 4C), which are in similar ranges to previous reports (Halm et al., 2009;  
340 Marcarelli & Wurtsbaugh, 2006, 2009; Rahav et al., 2022). Note, data on N<sub>2</sub> fixation  
341 rates in freshwater environments is still limited (Marcarelli et al., 2022). Normalizing  
342 these rates to the number of diazotrophs detected by immunolabeling flow cytometry  
343 resulted in N<sub>2</sub> fixation per cells that ranged between 0.3-88 attomole N cell<sup>-1</sup>. These  
344 specific rates were found to be significantly lower at the Sea of Galilee Lake or the  
345 Jordan River than the Mediterranean Sea. Previous studies indicated on high specific  
346 rates correspond to high C:N or N:P ratios (Inomura et al., 2018; Knapp et al., 2012),  
347 conditions that are often found in the Mediterranean Sea. Differently, it was recently  
348 reported that N<sub>2</sub> fixation rates per cell were high while at the same time nitrate  
349 concentrations in the surrounding environment were high (~2 μM) (Mills et al., 2020),  
350 conditions that could potentially impair diazotrophy. Currently, the cellular  
351 mechanisms that control N<sub>2</sub> fixation rates in environmental samples is not decisive  
352 and likely change according to the abiotic conditions and the different metabolic  
353 pathways.





354

355 **Figure 4.** Representative density plots of an immunolabeled subsample (Green as a  
356 function of SSC) that was collected from the Sea of Galilee Lake (A). Complimentary  
357 CLSM image was further captured from a lake subsample (A, top circle), whereas  
358 diazotrophs were identified by nitrogenase immunolabeling (Green), while total  
359 bacteria were detected by DAPI (Blue). The image scale bar is 10  $\mu m$ . Bacteria and  
360 diazotroph counts (BA and DA, respectively) were determined from the Sea of  
361 Galilee Lake, the Jordan River and the Mediterranean Sea (B).  $N_2$  fixation rates were  
362 measured from the same natural environments (C).  $N_2$  fixation per cell was calculated  
363 by normalizing the rates to number of DA.

364

## 365 Conclusion

366 Coupling immunolabeling and flow cytometry can be used to quantify the number of  
367 unicellular diazotrophs that synthesized the nitrogenase enzyme, thus were likely  
368 fixing  $N_2$ . This approach can be applied to count diazotrophs in controlled lab-scale  
369 experiments as well as various aquatic environments. Counting the total and  
370 immunolabeled cells of a diazotrophic monoculture indicated that even under  
371 anaerobic and N limiting conditions, only a fraction (15-20%) has synthesized the  
372 nitrogenase enzyme. That difference was likely due to the experimental conditions  
373 and yet highlights the importance of counting diazotrophs (even from monocultures

374 under controlled conditions) to determine fundamental aspects such as specific N<sub>2</sub>  
375 fixation per cell.

376 This approach can also enable quantification of unicellular diazotrophs in various  
377 marine and freshwater environments. Although the scope of this research was  
378 developing a new quantification approach for diazotrophs, it was interesting to find  
379 that N<sub>2</sub> fixation per cell was highest in the oligotrophic Mediterranean Sea, compared  
380 to the Jordan River and the Sea of Galilee Lake, pointing on their potential  
381 significance for total biological N production.

382 It should be highlighted that this approach should be further investigated and  
383 developed: (i) differentiating and specifically counting unicellular heterotrophic or  
384 phototrophic diazotrophs is of high interest to estimate their contribution to total N<sub>2</sub>  
385 fixation; (ii) the number of diazotrophs using this immunolabeled flow cytometry  
386 approach should be further compared to molecular-based approaches that are  
387 currently applied at various aquatic environments. Nevertheless, we suggest that  
388 adopting this approach could provide information on specific N<sub>2</sub> fixation capacity of  
389 freshwater and marine diazotrophs. Moreover, quantifying diazotrophs will likely  
390 provide new insights on the contribution of these microorganisms to the aquatic  
391 nitrogen cycle.

392

### 393 **Acknowledgments**

394 This paper is in partial fulfillment of EG Ph.D thesis at Ben Gurion University of the  
395 Negev. EB-Z thank the Israeli Science Foundation (grant number 944\21) for the  
396 supported of this project.

397

398 **Supporting information**

399 A full recipe of brackish water is available for read. We also provided tests about  
400 washing efficiency of bacteria and quality control of EA-IRMS. Additional images of  
401 immunolabeled bacteria are also provided.

402

403 **References**

404 Benavides M, Duhamel S, van Wambeke F, Shoemaker KM, Moisander PH, Salamon  
405 E, Riemann L, Bonnet, S (2020). Dissolved organic matter stimulates N<sub>2</sub> fixation  
406 and *nifH* gene expression in *Trichodesmium*. *FEMS Microbiology Letters*, 367,  
407 *fnaa034*. <https://doi.org/10.1093/femsle/fnaa034>

408 Bergman, B, Sandh G, Lin S, Larsson J, Carpenter, EJ (2013). *Trichodesmium* - a  
409 widespread marine cyanobacterium with unusual nitrogen fixation properties.  
410 *FEMS Microbiology Reviews*, 37, 285-302. [https://doi.org/10.1111/j.1574-](https://doi.org/10.1111/j.1574-6976.2012.00352)  
411 [6976.2012.00352](https://doi.org/10.1111/j.1574-6976.2012.00352).

412 Bertics VJ, Sohm, JA, Treude, T, Chow CET, Capone, DG, Fuhrman JA, & Ziebis W  
413 (2010). Burrowing deeper into benthic nitrogen cycling: The impact of  
414 Bioturbation on nitrogen fixation coupled to sulfate reduction. *Marine Ecology*  
415 *Progress Series*, 409, 1–15. <https://doi.org/10.3354/meps08639>

416 Bogler A, Bar-Zeev, E (2018). Membrane distillation biofouling: Impact of feedwater  
417 temperature on biofilm characteristics and membrane performance.  
418 *Environmental Science and Technology*, 52, 10019–10029.  
419 <https://doi.org/10.1021/acs.est.8b02744>

- 420 Bombar D, Paerl RW, Riemann L (2016). Marine non-cyanobacterial diazotrophs:  
421 moving beyond molecular detection. *Trends in Microbiology*, 24, 916–927.  
422 <https://doi.org/10.1016/j.tim.2016.07.002>
- 423 Chelius MK, & Triplett EW (2000). Immunolocalization of Dinitrogenase Reductase  
424 Produced by *Klebsiella pneumoniae* in Association with *Zea mays* L. *Applied*  
425 *and Environmental Microbiology*, 66, 783-787.  
426 <https://doi.org/10.1128/AEM.66.2.783-787.2000>
- 427 Currin CA, Paerl HW, Suba, GK, Alberte, RS (1990). Immunofluorescence detection  
428 and characterization of nitrogen-fixing microorganisms from aquatic  
429 environments. *Limnol Oceanogr*, 35, 59–71.  
430 <https://doi.org/10.4319/lo.1990.35.1.0059>
- 431 Feng X, Bandyopadhyay A, Berla B, Page L, Wu B, Pakrasi HB, Tang YJ (2010).  
432 Mixotrophic and photoheterotrophic metabolism in *Cyanothece* sp. ATCC 51142  
433 under continuous light. *Microbiology*, 156, 2566–2574.  
434 <https://doi.org/10.1099/mic.0.038232-0>
- 435 Foster RA, Subramaniam A, Mahaffey C, Carpenter EJ, Capone DG, Zehr JP (2007).  
436 Influence of the Amazon River plume on distributions of free-living and  
437 symbiotic cyanobacteria in the western tropical north Atlantic. *Limnology and*  
438 *Oceanography*, 52, 517-532. <https://doi.org/10.4319/lo.2007.52.2.0517>
- 439 Geisler E, Bogler A, Rahav E, Bar-Zeev E (2019). Direct detection of heterotrophic  
440 diazotrophs associated with planktonic aggregates. *Scientific Reports*, 9, 9288.  
441 <https://doi.org/10.1038/s41598-019-45505-4>
- 442 Gruber, N., & Galloway, J. N. (2008). An Earth-system perspective of the global  
443 nitrogen cycle. *Nature*, 451, 293–296. <https://doi.org/10.1038/nature06592>.

- 444 Halm H, Musat N, Lam P, Langlois R, Musat F, Peduzzi S, Lavik G, Schubert CJ,  
445 Singha B, Laroche J, Kuypers MMM (2009). Co-occurrence of denitrification  
446 and nitrogen fixation in a meromictic lake, Lake Cadagno (Switzerland).  
447 *Environmental Microbiology*, *11*, 1945–1958. [https://doi.org/10.1111/j.1462-](https://doi.org/10.1111/j.1462-2920.2009.01917)  
448 [2920.2009.01917](https://doi.org/10.1111/j.1462-2920.2009.01917).
- 449 Hoffman BM, Lukoyanov D, Yang ZY, Dean DR, Seefeldt LC (2014). Mechanism of  
450 nitrogen fixation by nitrogenase: The next stage. In *Chemical Reviews* *114*,  
451 4041–4062. <https://doi.org/10.1021/cr400641>.
- 452 Inomura K, Bragg J, Riemann L, Follows MJ (2018). A quantitative model of  
453 nitrogen fixation in the presence of ammonium. *PLoS ONE*, *13*, 1–16.  
454 <https://doi.org/10.1371/journal.pone.0208282>
- 455 Knapp AN, Dekaezemacker J, Bonnet S, Sohm JA, Capone DG (2012). Sensitivity of  
456 *Trichodesmium erythraeum* and *Crocospaera watsonii* abundance and N<sub>2</sub>  
457 fixation rates to varying NO<sub>3</sub><sup>-</sup> and PO<sub>4</sub><sup>3-</sup> concentrations in batch cultures. *Aquatic*  
458 *Microbial Ecology*, *66*(3), 223–236. <https://doi.org/10.3354/ame01577>
- 459 Lin S, Henze S, Lundgren P, Bergman B, & Carpenter EJ (1998). Whole-cell  
460 immunolocalization of nitrogenase in marine diazotrophic cyanobacteria,  
461 *Trichodesmium* spp. †. *Applied and Environmental Microbiology*, *64*, 3052-  
462 3058. <https://doi.org/10.1128/AEM.64.8.3052-3058.1998>
- 463 Luo YW, Shi D, Kranz SA, Hopkinson BM, Hong H, Shen R, Zhang F (2019).  
464 Reduced nitrogenase efficiency dominates response of the globally important  
465 nitrogen fixer *Trichodesmium* to ocean acidification. *Nature Communications*,  
466 *10*, 1521. <https://doi.org/10.1038/s41467-019-09554-7>

- 467 Marcarelli AM, Fulweiler RW, Scott JT (2022). Nitrogen fixation: A poorly  
468 understood process along the freshwater-marine continuum. *Limnology and*  
469 *Oceanography Letters*, 7, 1–10. <https://doi.org/10.1002/lol2.10220>
- 470 Marcarelli AM, Wurtsbaugh WA (2006). Temperature and nutrient supply interact to  
471 control nitrogen fixation in oligotrophic streams: An experimental examination.  
472 *Limnology and Oceanography*, 51, 2278–2289.
- 473 Marcarelli, A. M., & Wurtsbaugh, W. A. (2009). Nitrogen fixation varies spatially  
474 and seasonally in linked stream-lake ecosystems. *Biogeochemistry*, 94, 95–110.  
475 <https://doi.org/10.1007/s10533-009-9311-2>
- 476 Mills MM, Turk-Kubo KA, van Dijken GL, Henke BA, Harding K, Wilson ST,  
477 Arrigo KR, Zehr, JP (2020). Unusual marine cyanobacteria/haptophyte  
478 symbiosis relies on N<sub>2</sub> fixation even in N-rich environments. *ISME Journal*, 14,  
479 2395–2406. <https://doi.org/10.1038/s41396-020-0691-6>
- 480 Montoya JP, Voss M, Kahler P, Capone DG (1996). A Simple, high-precision, high-  
481 sensitivity tracer assay for N<sub>2</sub> fixation. *Applied and Environmental Microbiology*,  
482 62, 986–993. <https://doi.org/10.1128/aem.62.3.986-993.1996>
- 483 Rahav E, Giannetto MJ, Bar-Zeev E (2016). Contribution of mono and  
484 polysaccharides to heterotrophic N<sub>2</sub> fixation at the eastern Mediterranean  
485 coastline. *Scientific Reports*, 6, 27858. [https://doi.org/DOI: 10.1038/srep27858](https://doi.org/DOI:10.1038/srep27858)
- 486 Rahav E, Herut B, Spungin D, Levi A, Mulholland MR, Berman-Frank I (2022).  
487 Heterotrophic bacteria outcompete diazotrophs for orthophosphate in the  
488 Mediterranean Sea. *Limnology and Oceanography*, 67, 159–171.  
489 <https://doi.org/10.1002/lno.11983>

- 490 Riemann L, Farnelid H, Steward GFG (2010). Nitrogenase genes in non-  
491 cyanobacterial plankton: Prevalence, diversity and regulation in marine waters.  
492 *Aquatic Microbial Ecology*, 61, 235–247. <https://doi.org/10.3354/ame01431>
- 493 Riemann L, Rahav E, Passow U, Grossart HP, de Beer D, Klawonn I, Eichner M,  
494 Benavides M, Bar-Zeev E (2022). Planktonic aggregates as hotspots for  
495 heterotrophic diazotrophy: The plot thickens. *Frontiers in Microbiology*, 13,  
496 875050. <https://doi.org/10.3389/fmicb.2022.875050>
- 497 Spungin D, Pfreundt U, Berthelot H, Bonnet S, AlRoumi D, Natale F, Hess WR,  
498 Bidle KD, Berman-Frank I (2016). Mechanisms of *Trichodesmium* demise  
499 within the New Caledonian lagoon during the VAHINE mesocosm experiment.  
500 *Biogeosciences*, 13, 4187–4203. <https://doi.org/10.5194/bg-13-4187-2016>
- 501 Turk, KA, Rees AP, Zehr JP, Pereira N, Swift P, Shelley R, Lohan M, Woodward E  
502 MS, Gilbert J (2011). Nitrogen fixation and nitrogenase (*nifH*) expression in  
503 tropical waters of the eastern North Atlantic. *ISME Journal*, 5, 1201–1212.  
504 <https://doi.org/10.1038/ismej.2010.205>
- 505 White AE, Granger J, Selden C, Gradoville MR, Potts L, Bourbonnais A, Fulweiler  
506 RW, Knapp AN, Mohr W, Moisander PH, Tobias CR, Caffin M, Wilson ST,  
507 Benavides M, Bonnet S, Mulholland MR, Chang BX (2020). A critical review of  
508 the  $^{15}\text{N}_2$  tracer method to measure diazotrophic production in pelagic ecosystems.  
509 *Limnology and Oceanography: Methods*, 18, 129-147.  
510 <https://doi.org/10.1002/lom3.10353>
- 511 Zehr JP (2011). Nitrogen fixation by marine cyanobacteria. *Trends in Microbiology*,  
512 19, 162–173. <https://doi.org/10.1016/j.tim.2010.12.004>

513 Zehr JP, Capone DG (2020). Changing perspectives in marine nitrogen fixation.

514 *Science*, 368, 1–11. <https://doi.org/10.1126/science.aay9514>

515 Zulkefli, NS, Hwang SJ (2020). Heterocyst development and diazotrophic growth of

516 *anabaena variabilis* under different nitrogen availability. *Life*, 10, 279.

517 <https://doi.org/10.3390/life10110279>

518

519

520